

Summertime "ozone valley" over the Tibetan Plateau derived from ozonesondes and EP/TOMS data

メタデータ	言語: eng 出版者: 公開日: 2017-10-03 キーワード (Ja): キーワード (En): 作成者: メールアドレス: 所属:
URL	http://hdl.handle.net/2297/12578

1 Summertime ‘ozone valley’ over the Tibetan Plateau derived from
2 ozonesondes and EP/TOMS data

3

4 Yutaka Tobo,¹ Yasunobu Iwasaka,¹ Daizhou Zhang,² Guangyu Shi,³ Yoon-Suk
5 Kim,⁴ Koichi Tamura,⁴ and Tetsuya Ohashi⁴

6

7 ¹Frontier Science Organization, Kanazawa University, Kanazawa 920-1192,
8 Japan

9 ²Faculty of Environmental and Symbiotic Sciences, Prefectural University of
10 Kumamoto, Kumamoto 862-8502, Japan

11 ³Institute of Atmospheric Physics, Chinese Academy of Science, Beijing 100029,
12 China

13 ⁴Solar-Terrestrial Environment Laboratory, Nagoya University, Nagoya
14 464-8601, Japan

1 **Abstract**

2

3 During the Asian summer monsoon period, total ozone over the Tibetan
4 Plateau is much lower than that over the surrounding areas when compared at
5 the same latitudes. This phenomenon called the “ozone valley” was investigated
6 continuously with the use of ozonesondes and Earth Probe/Total Ozone Mapping
7 Spectrometer (EP/TOMS). These measurements reveal that although relatively
8 low ozone mixing ratios extend from the troposphere to the lower stratosphere,
9 those near the tropopause (between about 150 and 70 hPa) largely contribute to
10 lower total ozone over the Tibetan Plateau. Temperatures near the tropopause
11 appear to be correlated with the observed ozone changes. Meteorological
12 analyses show that this phenomenon is accompanied by the upper level monsoon
13 anticyclone, which is characterized by deep convection over South Asia. These
14 results suggest that lower ozone mixing ratios and colder temperatures near the
15 tropopause are primarily due to convection, which is linked to the Asian summer
16 monsoon.

1 **1. Introduction**

2
3 Total column ozone over mountainous areas is relatively low as compared to
4 non-mountainous areas at the same latitudes. The Tibetan Plateau has an average
5 elevation of >4000 meters and occupies an area of about 2.5 million square
6 kilometers in South Asia. Hence one would expect low total ozone over the
7 Tibetan Plateau to be associated with missing the integrated ozone columns from
8 the mountain to non-mountain ground surfaces. However, it is evident that the
9 negative deviations from the zonal mean total ozone are much larger in summer
10 than in winter, indicating summertime decreases in total ozone over the Tibetan
11 Plateau [*Zhou and Luo, 1994; Zou, 1996*]. This regional phenomenon found in
12 summer is dubbed the “ozone valley”. The ozone valley is small in scale as
13 compared to the Antarctic “ozone hole”, but major in radiative effect; because
14 the ozone valley is formed in summertime when the Tibetan Plateau and its
15 residents are exposed to extra strong sunlight.

16 The mechanisms responsible for the low total ozone have been discussed for
17 decades. In particular, the possibility of linkages between ozone and the Asian
18 summer monsoon circulation is of interest. During summer, the elevated surface
19 heating and rising air over the Tibetan Plateau lead to anticyclonic circulation
20 and divergence in the upper troposphere and lower stratosphere [*Yanai et al.,*
21 *1992*]. The upper level monsoon anticyclone (i.e., Tibetan anticyclone) exhibits
22 intraseasonal variability and travels to and fro between two preferred regions,
23 namely the Tibetan Plateau and the Iranian Plateau [*Zhang et al., 2002*]. Recent
24 satellite measurements and model studies have focused on the importance of the
25 Tibetan anticyclone and its coupling to deep convection that has the potential to
26 transport ozone-poor air from the boundary layer into the upper troposphere and
27 also lower stratosphere [*Gettelman et al., 2004; Randel and Park, 2006; Park et*
28 *al., 2007*].

1 The height dependence of the ozone changes is important for understanding
2 mechanisms responsible for the occurrence of the ozone valley over the Tibetan
3 Plateau; however, few in-situ measurements have documented it. In this study,
4 we present total ozone and ozonesonde measurements of the ozone valley over
5 the Tibetan Plateau in the summer of 1999. We show that minima in total ozone
6 are linked to the development of the Tibetan anticyclone, and relatively low
7 ozone mixing ratios extend to the lowermost stratosphere as well as troposphere.
8 These results raise the possibility that deep convection could primarily affect
9 ozone mixing ratios and hence temperatures near the tropopause.

11 **2. Data and Analyses**

13 Time series of total column ozone are obtained from the Earth Probe/Total
14 Ozone Mapping Spectrometer (EP/TOMS) version 8 operated by the National
15 Aeronautics Space Administration/Goddard Space Flight Center (NASA/GSFC).
16 The EP/TOMS dataset uses a horizontal resolution of 1° latitude \times 1.25°
17 longitude. The unit for total ozone is Dobson Unit (DU; 1 DU is defined as 0.01
18 mm thickness at 1°C and 1 atmospheric pressure). More information is available
19 at http://toms.gsfc.nasa.gov/eptoms/ep_v8.html.

20 In addition, a detailed analysis of the vertical structure of the ozone changes
21 is performed by using balloon-borne measurements in the summer of 1999 at
22 Lhasa (29.7°N , 91.1°E , 3650 meters above sea level), located in the southern
23 part of the Tibetan Plateau. The ozone and temperature profiles were measured
24 with an electrochemical concentration cell (ECC) ozonesonde and radiosonde.
25 Here we use the results for 18-25 August 1999 (no available data on 20 August
26 1999). For the purpose of comparison with non-mountainous areas at similar
27 latitudes, we refer to the monthly mean ozone and temperature profiles derived
28 from systematic balloon-borne measurements at Kagoshima (31.6°N , 130.5°E ,

1 31 meters above sea level), located in the southwestern part of Japan. Note that
2 Japanese KC96 ozonesondes are used for ozone measurements at Kagoshima.
3 According to *Deshler et al.* [2008], the KC96 ozonesondes tend to underestimate
4 ozone while the ECC ozonesondes overestimate. The precisions are about 5-15%
5 at pressures >30 hPa.

6 This study also uses horizontal wind fields retrieved from the National
7 Centers for Environmental Prediction/National Center for Atmospheric Research
8 (NCEP/NCAR) daily reanalysis data [*Kalnay et al.*, 1996], available with a
9 horizontal resolution of 2.5° latitude \times 2.5° longitude and 17 pressure levels
10 from 1000 to 10 hPa. The NCEP/NCAR reanalysis data is used to investigate the
11 development and motion of the anticyclone in the upper troposphere and lower
12 stratosphere. In addition, the Hybrid Single-Particle Lagrangian Integrated
13 Trajectory (HYSPLIT) model (<http://www.arl.noaa.gov/ready/hysplit4.html>) is
14 used to quantify the backward trajectories for the observation period.

15

16 **3. Specification of Low Ozone Event**

17

18 Figures 1a and 1b illustrate the geographical distributions of total ozone
19 averaged for 18-22 August and for 23-27 August 1999, respectively. Figure 1a
20 shows observable minima in total ozone over the Tibetan Plateau at 80° - 100° E,
21 indicating the occurrence of the ozone valley. Horizontal wind fields at 100 hPa
22 (near-tropopause) are also plotted in the figures. The meteorological analysis
23 indicates that a synoptic-scale anticyclone was initially located over the Tibetan
24 Plateau and coherent with minimum total ozone there. After that, the anticyclone
25 started to move to the westward and then developed over the Iranian Plateau at
26 50° - 70° E (Figure 1b). The changes in total ozone were linked to the movement
27 of the anticyclone. Following the movement, total ozone in the vicinity of the
28 Tibetan Plateau showed an increase and that of the Iranian Plateau exhibited a

1 decrease.

2 Figure 2 show the vertical profiles of ozone mixing ratios at Lhasa during
3 18-25 August 1999, along with the monthly mean profiles of ozone mixing ratios
4 at Kagoshima. There are some differences in the details of the shapes of these
5 profiles. The balloon flights on 18-22 August 1999 were conducted within the
6 Tibetan anticyclone. In these cases, there were little differences in tropospheric
7 ozone mixing ratios between Lhasa and Kagoshima (note that Kagoshima is
8 surrounded by sea and therefore frequently influenced by ozone-poor air). More
9 importantly, relatively low ozone mixing ratios over Lhasa extended over broad
10 layers ranging approximately to 70 hPa.

11 The Tibetan anticyclone occurs primarily as a response to diabatic heating
12 associated with deep convection over South Asia during summer [*Yanai et al.*,
13 1992]. In cases where the anticyclonic circulation was formed over the Tibetan
14 Plateau, temperatures from the ground surface to about 150 hPa over Lhasa was
15 always higher than those over Kagoshima (Figure 2), suggesting an increase in
16 diabatic heating and enhanced convection over the Plateau. This tropospheric
17 warming leads to the reversal of meridional temperature gradient on the south of
18 the Plateau [*Yanai et al.*, 1992]. As a result, tropospheric ozone abundances over
19 Lhasa during the low ozone event could be the result of the arrival of air masses
20 transporting ozone-poor air from the Bay of Bengal and the Arabian Sea (see
21 backward trajectories starting on 21-22 August 1999 in Figure 3). Also, given
22 the occurrence of the anticyclone during the low ozone event, it is assumed that
23 relatively low ozone mixing ratios near the tropopause are caused by the upward
24 transport of ozone-poor air in deep convective systems.

25 After 24 August 1999, the Tibetan Plateau was located at the eastern edge of
26 the anticyclone and thus it is expected that convectively suppressed conditions
27 prevailed over Lhasa. During this period, relatively high ozone mixing ratios
28 were found from the ground surface to about 250 hPa (Figure 2). The air mass

1 trajectories changed to pass over inland China (see backward trajectories starting
2 on 24-25 August 1999 in Figure 3), indicating that the tropospheric ozone-rich
3 air originated from continental sources. Ozonesonde measurements at Xining
4 (36.4°N, 101.5°E, 2296 meters above sea level), located in the northeastern part
5 of the Tibetan Plateau, show tropospheric ozone mixing ratios of >60 ppbv
6 under normal summertime conditions [Zheng *et al.*, 2004]. Thus, the relatively
7 high ozone mixing ratios measured at Lhasa on 24-25 August 1999 are similar to
8 those at Xining. In addition, the 25 August flight showed ozone recovery in the
9 lowermost stratosphere, and as a consequence, negative ozone anomalies near
10 the tropopause extended only to about 90 hPa. The 18 September flight that was
11 conducted at the eastern edge of the anticyclone also indicated ozone recovery
12 probably resulting from convectively suppressed conditions over the Plateau.

13 Figure 4a shows the integrated column ozone between 600 and 70 hPa based
14 on ozonesonde measurements at Lhasa during 18-25 August 1999. This figure
15 also includes time series of the EP/TOMS total ozone over Lhasa in August 1999.
16 These data show that the total ozone over Lhasa was largely influenced by ozone
17 variations between 600 and 70 hPa. We further divide the integrated column
18 ozone into three altitudes and examine the local ozone anomalies (deviations
19 from the monthly mean ozone at Kagoshima). The results shown in Figures 4b,
20 4c, and 4d indicate the ozone valley to be a localized phenomenon that extends
21 from about 150 to 70 hPa.

22

23 **4. Temperature Changes near the Tropopause**

24

25 The vertical profiles of temperatures at Lhasa during the observation period
26 in this study are shown in Figure 2, together with the monthly mean data at
27 Kagoshima. The local temperature anomalies (deviations from the monthly mean
28 temperatures at Kagoshima) appeared most frequently over narrow layers near

1 the tropopause between about 130 and 70 hPa. When the anticyclone developed
2 over the Tibetan Plateau, cold temperature anomalies of about 5-10 K occurred
3 near the tropopause. On the other hand, when the anticyclone shifted to the west,
4 the anomalies were small. Thus, the temperature changes show patterns very
5 similar to the observed ozone changes near the tropopause. Also, as shown in
6 Figure 5, it seems likely that the temperatures vary with changes in the ozone
7 mixing ratios.

8

9 **5. Summary and Discussion**

10

11 Synoptic analyses of total column ozone and meteorological conditions have
12 demonstrated that the occurrence of the ozone valley over the Tibetan Plateau is
13 closely linked to the anticyclone in the upper troposphere and lower stratosphere
14 (Figure 1). In addition, ozonesonde measurements at Lhasa have provided new
15 information relevant to the vertical structure of the ozone valley. The vertical
16 profiles of ozone mixing ratios within the Tibetan anticyclone indicate relatively
17 low ozone mixing ratios extending to 70 hPa (Figure 2), suggesting that the
18 anticyclone and its coupling to deep convection influences lower stratospheric
19 as well as tropospheric ozone abundances over the Tibetan Plateau. The negative
20 ozone anomalies near the tropopause between about 150 and 70 hPa largely
21 contribute to a reduction in total ozone over the Tibetan Plateau (Figure 4).

22 The relatively low ozone near the tropopause is primarily attributed to the
23 upward transport of ozone-poor air in deep convective systems. Other satellite
24 and model studies have also suggested minima in ozone mixing ratios within the
25 monsoon anticyclone [Gettelman *et al.*, 2004; Randel and Park, 2006; Park *et*
26 *al.*, 2007], which they attribute to seasonal changes in dynamics in the monsoon
27 region. On the other hand, it has been reported that there are relatively high
28 values of water vapor [Gettelman *et al.*, 2004; Fu *et al.*, 2006; Randel and Park,

1 2006; *Park et al.*, 2004, 2007], methane, and NO_x ($= \text{NO} + \text{NO}_2$) [*Park et al.*,
2 2004] near the summertime tropopause. The occurrence of cirrus clouds has also
3 been observed [*Fu et al.*, 2006; *Tobo et al.*, 2007]. Other processes related to
4 these species may have an affect on ozone abundances in the upper troposphere
5 and lower stratosphere, and thus further investigations are needed to account for
6 these sensitivities.

7 The present results have indicated that temperatures near the tropopause are
8 strongly correlated with the observed ozone changes (Figure 5). It is likely that
9 cold temperature anomalies within the anticyclone at 100 hPa are primarily a
10 dynamical response to enhanced convection [*Park et al.*, 2007]. Although we
11 consider that the ozone changes have only a small effect on the energy budget of
12 the tropopause, the reduction in ozone mixing ratios near the tropopause may
13 reduce the radiative heating rate. Thus, comprehensive model studies as well as
14 measurements of ozone and other greenhouse gases are needed to explain the
15 mechanisms for the coupled temperature-ozone changes.

1 **Acknowledgements**

2

3 We thank D. J. SuoLang and the staff members of the Meteorological Bureau
4 of Tibet Autonomous Region for their technical supports in the fieldwork. We
5 also thank to the Japan Meteorological Agency for providing sonde data at
6 Kagoshima, and Katsuya Yamashita of the Meteorological Research Institute for
7 his helpful supports necessary for extensive discussions. This research was
8 funded by the Japan Ministry of Education, Culture, Sports, Science and
9 Technology (PI: Yasunobu Iwasaka, No.10144104 & No.10041115), National
10 Natural Science Foundation of China (PI: Guangyu Shi, No.49775275), and
11 21st-Century COE program of Kanazawa University (PI: Kazuichi Hayakawa).

1 **References**

2

3 Deshler, T., J. L. Mercer, H. G. J. Smit, R. Stubi, G. Levrat, B. J. Johnson, S. J.
4 Oltmans, R. Kivi, A. M. Thompson, J. Witte, J. Davies, F. J. Schmidlin, G.
5 Brothers, and T. Sasaki (2008), Atmospheric comparison of electrochemical cell
6 ozonesondes from different manufacturers, and with different cathode solution
7 strengths: The Balloon Experiment on Standards for Ozonesondes, *J. Geophys.*
8 *Res.*, *113*, D04307, doi:10.1029/2007JD008975.

9

10 Fu, R., Y. Hu, J. S. Wright, J. H. Jiang, R. E. Dickinson, M. Chen, M. Filipiak,
11 W. G. Read, J. W. Waters, and D. L. Wu (2006), Short circuit of water vapor and
12 polluted air to the global stratosphere by convective transport over the Tibetan
13 Plateau, *Proc. Natl. Acad. Sci. U. S. A.*, *103*, 5664-5669.

14

15 Gettelman, A., D. E. Kinnison, T. J. Dunkerton, and G. P. Brasseur (2004),
16 Impact of monsoon circulations on the upper troposphere and lower stratosphere,
17 *J. Geophys. Res.*, *109*, D22101, doi:10.1029/2004JD004878.

18

19 Kalnay, E., M. Kanamitsu, R. Kister, W. Collins, D. Deaven, L. Gandin, M.
20 Iredell, S. Saha, G. White, J. Woollen, Y. Zhu, M. Chelliah, W. Ebisuzaki, W.
21 Higgins, J. Janowiak, K. C. Mo, C. Ropelewski, J. Wang, A. Leetmaa, R.
22 Reynolds, R. Jenne, and D. Joseph (1996), The NCEP/NCAR 40-year reanalysis
23 project, *Bull. Am. Meteorol. Sci.*, *77*, 437-471.

24

25 Park, M., W. J. Randel, A. Gettelman, S. T. Massie, and J. H. Jiang (2007),
26 Transport above the Asian summer monsoon anticyclone inferred from Aura
27 Microwave Limb Sounder tracers, *J. Geophys. Res.*, *112*, D16309,
28 doi:10.1029/2006JD008294.

1
2 Park, M., W. J. Randel, D. E. Kinnison, R. R. Garcia, and W. Choi (2004),
3 Seasonal variation of methane, water vapor, and nitrogen oxide near the
4 tropopause: Satellite observations and model simulations, *J. Geophys. Res.*, *109*,
5 D03302, doi:10.1029/2003JD003706.
6
7 Randel, W. J., and M. Park (2006), Deep convective influence on the Asian
8 summer monsoon anticyclone and associated tracer variability observed with
9 Atmospheric Infrared Sounder (AIRS), *J. Geophys. Res.*, *111*, D12314,
10 doi:10.1029/2005JD006490.
11
12 Tobo, Y., D. Zhang, Y. Iwasaka, and G. Shi (2007), On the mixture of aerosols
13 and ice clouds over the Tibetan Plateau: Results of a balloon flight in the
14 summer of 1999, *Geophys. Res. Lett.*, *34*, L23801, doi:10.1029/2007GL031132.
15
16 Yanai, M., C. Li, and Z. Song (1992), Seasonal heating of the Tibetan Plateau
17 and its effects on the evolution of the Asian summer monsoon, *J. Meteorol. Sci.*
18 *Jpn.*, *70*, 319-351.
19
20 Zhang, Q., G. Wu, and Y. Qian (2002), The bimodality of the 100 hPa South Asia
21 High and its relationship to the climate anomaly over East Asia in summer, *J.*
22 *Meteorol. Sci. Jpn.*, *80*, 733-744.
23
24 Zheng, X., X. Zhou, J. Tang, Y. Qin, and C. Chan (2004), A meteorological
25 analysis on a low tropospheric ozone event over Xining, North Western China on
26 26-27 July 1996, *Atmos. Environ.*, *38*, 261-271.
27
28 Zhou, X., and C. Luo (1994), Ozone valley over Tibetan Plateau, *Acta Meteorol.*

1 *Sinica*, 8, 505-506.

2

3 Zou, H. (1996), Seasonal variation and trends of TOMS ozone over Tibet,

4 *Geophys. Res. Lett.*, 23, 1029-1032.

1 **Figure 1.** EP/TOMS total ozone maps averaged for 5 days; (a) 18-22 August
2 1999, (b) 23-27 August 1999. Also shown are NCEP/NCAR horizontal wind
3 fields at 100 hPa.

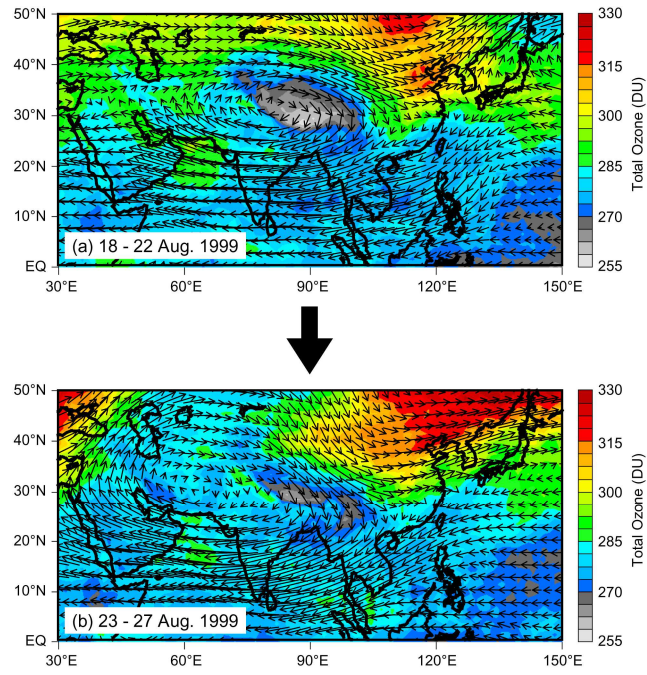
4
5 **Figure 2.** Vertical profiles of ozone mixing ratios and temperatures at Lhasa
6 obtained from ozonesondes on 18-25 August 1999 (without 20 August 1999) and
7 18 September 1999. Monthly mean ozone mixing ratios and temperatures at
8 Kagoshima are also shown.

9
10 **Figure 3.** HYSPLIT backward trajectory analyses from the measurement site
11 starting at 450 hPa on 21, 22, 24, and 25 August 1999 at 06:00 UTC. Dots on
12 each trajectory are plotted every 12 hours.

13
14 **Figure 4.** (a) Time series of column ozone integrated between 600 and 70 hPa
15 from ozonesondes and EP/TOMS total ozone at Lhasa in August 1999. Also
16 shown are the ozone anomalies (deviations from the monthly mean ozone data at
17 Kagoshima) divided into three altitudes; (b) 150-70 hPa, (c) 300-150 hPa, (d)
18 600-300 hPa.

19
20 **Figure 5.** Scatter diagram of ozone mixing ratios with temperatures at 100, 90,
21 and 80 hPa from ozonesondes at Lhasa for 18-25 August 1999 (without 20
22 August 1999). Data on 24 and 25 August 1999 are shown as shaded points.

1



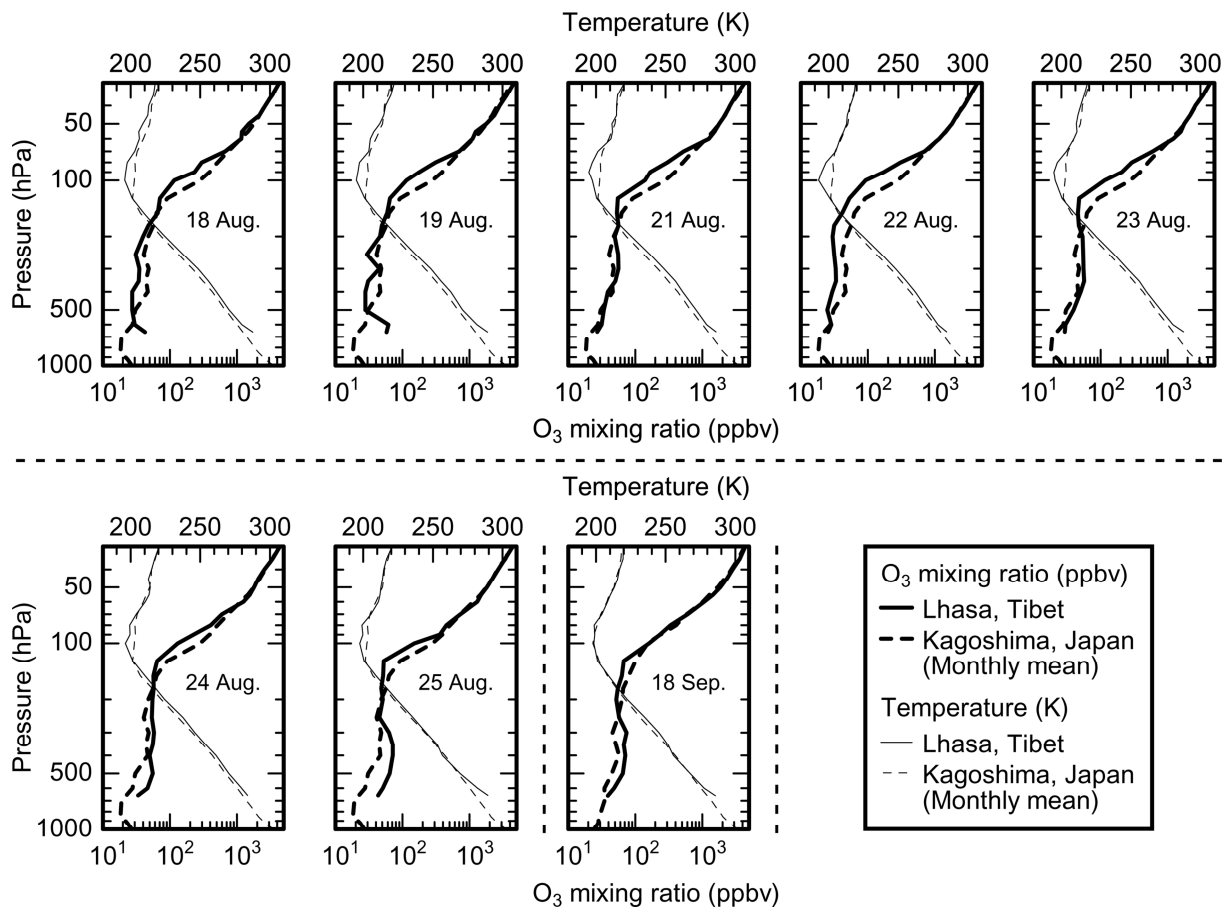
2

3

4

Figure 1

1



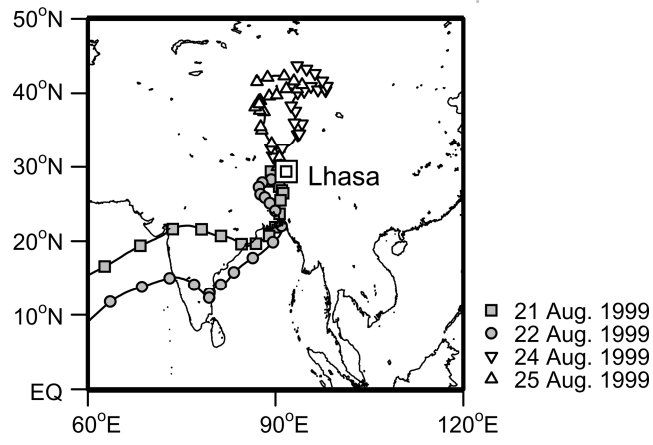
2

3

4

Figure 2

1



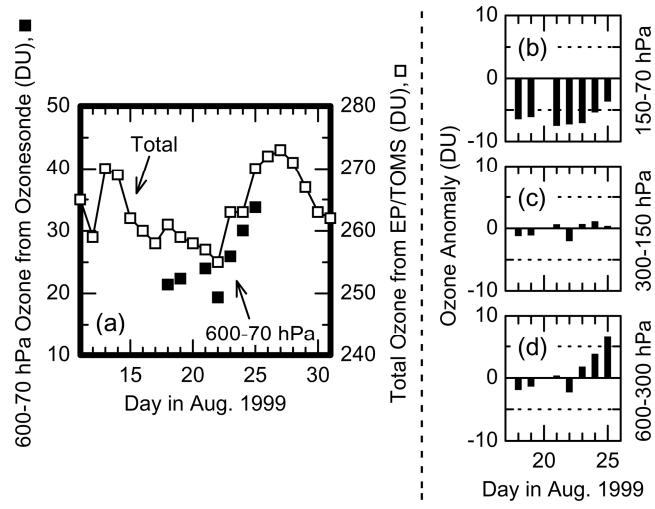
2

3

4

Figure 3

1



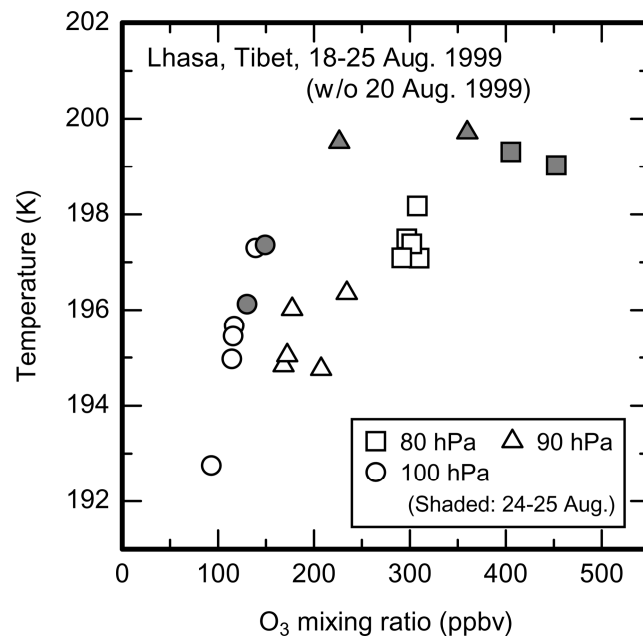
2

3

4

Figure 4

1



2

3

4

Figure 5